



# Electrochemical behaviour of aqueous SO<sub>2</sub> at polycrystalline gold electrodes in acidic media. A voltammetric and in-situ vibrational study. Part II. Oxidation of SO<sub>2</sub> on bare and sulphur-modified electrodes

C. Quijada<sup>a</sup>, E. Morallón<sup>b,1</sup>, J.L. Vázquez<sup>b,\*</sup>, L.E.A. Berlouis<sup>c</sup>

<sup>a</sup> *Departamento de Ingeniería Textil y Papelería, E.P.S.A., Universitat Politècnica de València, Paseo del Viaducto, 1, 03801 Alcoy, Spain*

<sup>b</sup> *Departamento de Química Física, Universidad de Alicante, Ap. 99, 03080 Alicante, Spain*

<sup>c</sup> *Department of Pure and Applied Chemistry, University of Strathclyde, 295 Cathedral Street, G1 1XL Glasgow, Scotland, UK*

Received 7 April 2000; received in revised form 14 July 2000

## Abstract

The electrochemical oxidation of SO<sub>2</sub> on polycrystalline gold electrodes has been studied by means of cyclic voltammetry and in situ vibrational techniques. On bare gold electrodes, SO<sub>2</sub> is irreversibly oxidised on forward scans at ~0.6 V/RHE, featuring a diffusion-limited peak. Oxidation is inhibited by the formation of chemisorbed oxygen. A SO<sub>2</sub> anodic current rise occurs on the reverse scan in parallel with the reduction of the metal oxide layers. As shown by FT-IR, oxidation proceeds to yield a mixture of soluble S(VI) species as stable reaction products. From vibrational spectra and results from the irreversible adsorption method, it follows that no strongly adsorbed S–O-like residues are present onto the gold surface in the region 0.3–0.5 V/RHE. On sulphur-modified electrodes improved electrocatalysis is manifested by the shift of the diffusion-limited peak to lower potentials. The best performance is observed at a sulphur coverage of 0.5. At higher coverage, sulphur adlayers impart lower catalytic efficiency and eventually show strong poisoning properties. This behaviour is exhibited by sulphur adlayers generated either in situ by SO<sub>2</sub> reduction or ex situ by sulphide adsorption/oxidation in acidic or alkaline media. © 2000 Elsevier Science Ltd. All rights reserved.

**Keywords:** Sulphur dioxide; Gold electrode; Platinum electrode; SER spectroscopy; FT-IR spectroscopy; Electrocatalysis; Flue gas desulphurisation

## 1. Introduction

In part I [1], the study of the reduction processes suffered by SO<sub>2</sub> at gold electrodes was undertaken. We presented therein voltammetric and vibrational evi-

dence to substantiate the production of a monomeric sulphur adlayer by reduction of SO<sub>2</sub> at 0.1 < E < 0.3 V/RHE and the subsequent deposition of polymeric sulphur after oxidation of soluble SO<sub>2</sub> reduction products formed at E < 0.1 V (tentatively identified as H<sub>2</sub>S<sub>x</sub>, x = 1, 2 ...). To complete the overall picture of the electrochemical reactivity of SO<sub>2</sub>, the investigation of the oxidation reaction is now addressed.

As for reduction, there is relatively little work devoted to the study of the SO<sub>2</sub> oxidation reaction on

\* Corresponding author. Tel.: +34-6-5903539; fax: +34-6-5903537.

E-mail address: jlvazquez@ua.es (J.L. Vázquez).

<sup>1</sup> ISE member.

gold, as compared to Pt. Seo and Sawyer [2] distinguished two modes for the electrochemical oxidation of  $\text{SO}_2$  on gold. The first was ascribed to a purely electrochemical charge-transfer process and the second to a chemical oxidation by electrochemically generated metal oxide. Their interest was chiefly directed at the mechanism of the electron-transfer process, whose diffusion character was established from the constancy of  $jx\tau^{1/2}$  data (chronopotentiometric experiments) and the linear relationship between the peak current and the square root of the sweep rate. Moreover, the number of electrons involved in the overall process was inferred to be two, so indicating an overall oxidation of  $\text{SO}_2$  to sulphate. Samec and Weber [3,4] claimed that the 'diffusion peak' reported by Seo and Sawyer has actually a complex shape, since two resolved voltammetric features can be perceived. The less positive peak does correspond to a diffusion-limited, two-electron oxidation of  $\text{SO}_2$ , which takes place through a weakly adsorbed species as an intermediate. The more positive peak however was associated with a surface process: the oxidative desorption of strongly adsorbed  $\text{SO}_2$ . Recent Surface Enhanced Raman Scattering (SERS) studies of roughened gold in contact with aqueous  $\text{SO}_2$  [5] revealed a band at  $1130\text{ cm}^{-1}$ , which was ascribed to adsorbed  $\text{SO}_2$ . More recent voltammetric and radiolabelling studies [6] postulated the formation of both SO-type species (presumably dithionate) and  $\text{HSO}_4^-/\text{SO}_4^{2-}$  upon electro-oxidation of S(IV)-containing solutions on gold at various pH. These oxidised species adsorb on the gold surface and apparently inhibit the oxidation of bulk  $\text{SO}_2$ .

The strong dependence on the nature of adsorbed species (and indirectly on the potential range explored) of the reproducibility and magnitude of the  $\text{SO}_2$  oxidation current is well documented for other noble metals such as platinum [7–11]. Thus, we focus herein our attention on the oxidative behaviour of aqueous  $\text{SO}_2$  on gold electrodes in the absence and the presence of sulphur adlayers. The influence of these adlayers on the electrode kinetics has been assessed by monitoring the peak current and peak potential of the  $\text{SO}_2$  oxidation feature. Sulphur adlayers with different properties and coverage were obtained in  $\text{SO}_2$ -containing solutions by cycling to various lower potential limits, chosen according to the reductive behaviour reported in an earlier paper [1]. The catalytic properties of sulphur adlayers formed by sulphide adsorption in acidic and alkaline media were also tested.

## 2. Experimental

The experimental set-up, reagents and electrodes employed for the voltammetric and spectroscopic experiments were fully described in part I of this series [1],

with the exception that a flat  $\text{CaF}_2$  window was used instead a prismatic one in FT-IR measurements. The employment of thinner flat windows permitted us to collect spectra with a better S/N ratio between 1100 and  $1000\text{ cm}^{-1}$ . Infrared spectra were typically collected with a  $8\text{-cm}^{-1}$  resolution and resulted from the average of 200 interferograms. SER spectra were gathered with a spectral resolution of  $2\text{ cm}^{-1}$  and at an exposure time of 10–50 s. The electrode potential was measured against a reversible hydrogen electrode. Unless otherwise stated, cyclic voltammograms were recorded at room temperature and at a sweep rate of  $50\text{ mV}^{-1}$ .

Sulphur dioxide solutions were made up by dissolving solid  $\text{Na}_2\text{SO}_3$  (Merck, analytical grade) into the acidic test solutions (10% v/v  $\text{H}_2\text{SO}_4$  or 0.5 M  $\text{HClO}_4$ ). The use of perchloric solutions was adopted in spectroscopic experiments to prevent interference from bulk hydrogen sulphate anions. In the spectroscopic runs, an aliquot from a 0.1 M S(IV) + 0.5 M  $\text{HClO}_4$  stock solution was spiked into the electrolyte-containing spectroelectrochemical cell [9,10]. The concentration of the electroactive species is referred to the total S(IV) initially dissolved. An inert atmosphere was maintained over the solution surface during all the measurements.

Sulphur adlayers were generated electrochemically by potential-controlled transformation of  $\text{SO}_2$  (or sulphide). Sulphur coverage was inferred from the charge passed during the stripping of the isolated adlayer. The isolation of the adlayer was carried out by withdrawal of the electrode from the  $\text{SO}_2$ - or sulphide-containing cell, rinsing with ultrapure water and transferral to a secondary cell filled with the background electrolyte [9,11].

## 3. Results and discussion

### 3.1. Oxidation of $\text{SO}_2$ on bare gold

The voltammetric shape for the oxidation of aqueous  $\text{SO}_2$  in the potential region from 0.50 to 1.75 V (first cycle) is shown in Fig. 1 for different S(IV) concentrations. The oxidation of  $\text{SO}_2$  begins at a potential of  $\sim 0.6\text{ V}$ , giving rise to a peak located between 0.75 and 0.85 V. This voltammetric feature is reminiscent in shape and position of those reported earlier [2–4], and can accordingly be attributed to a diffusion-limited oxidation process.

At the higher concentration (solid curve), the  $\text{SO}_2$  oxidation current undergoes a sharp drop from 1.4 V. This behaviour could be related an inhibition caused by the hindering of surface active sites by adsorbed oxygen [3,4], since the formation of surface metal oxide commences at  $\sim 1.4\text{ V}$ . However, the inhibition by surface oxide seems not to be complete, as evidenced at the lower S(IV) concentrations (long and short dashed

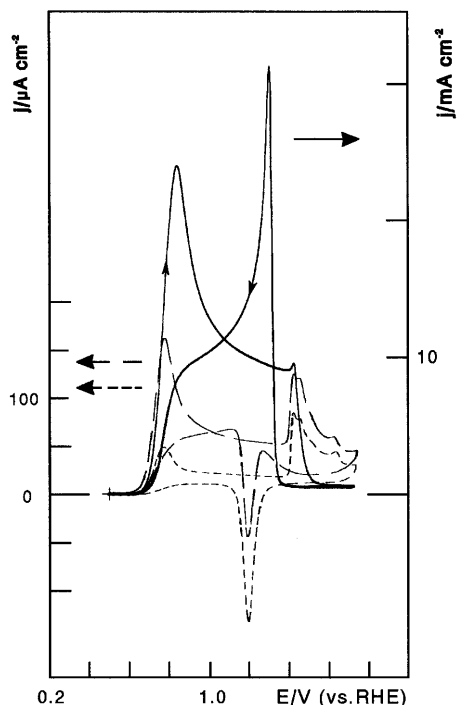


Fig. 1. Oxidation of  $\text{SO}_2$  on polycrystalline Au in 10%  $\text{H}_2\text{SO}_4$ ; 100 mM S(IV) (—); 1 mM S(IV) (---); and 0.5 mM (— · — · —).

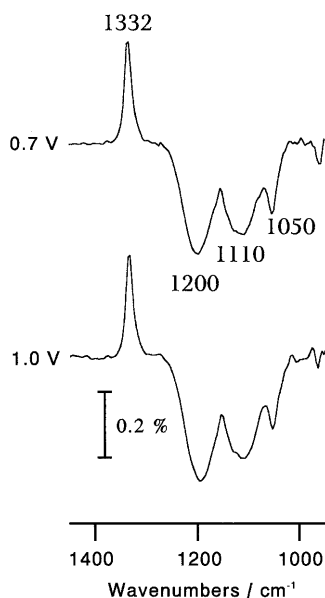


Fig. 2. In situ FT-IR spectra for the oxidation of  $\text{SO}_2$  ( $c_{\text{S(IV)}} \approx 10 \text{ mM}$ ) on polycrystalline Au in 0.5 M  $\text{HClO}_4$ . The reference spectrum was taken at 0.5 V. The sample was irradiated with p-polarised light.

lines), where the oxygen adsorption current is to a great extent superimposed onto the  $\text{SO}_2$  diffusion tail. This circumstance might correspond to the ability of  $\text{SO}_2$  to oxidise electrochemically on the oxide layer.

Sulphur dioxide also undergoes oxidation on gold electrodes during reverse sweeps. This effect is particularly remarkable at high S(IV) concentration (solid line), showing a sharp peak in the potential region where reduction of surface oxide occurs. The appearance of an anodic peak on negative scans is typical of oxidative processes inhibited by surface oxidation of the substrate [12,13]. The current decrease caused by the inhibiting surface process permits diffusion to restore the  $\text{SO}_2$  concentration profile. Thus, the increase in current observed upon reversing the scan is a consequence of the deinhibition of the surface as the metal oxide layer is stripped. A similar peaking behaviour on reverse sweeps was reported for the oxidation of  $\text{SO}_2$  on  $\text{SO}_2^-$  and S-covered Pt electrodes [9,10]. The difference in shape and magnitude of the reversal peak is likely to be caused by the different reduction rates of gold and platinum surface oxides. Moreover, it has been proposed [9] that the shape of the anodic peak in negative-going sweeps is additionally determined on Pt by the increasing adsorption of  $\text{SO}_2$  at potentials approaching 0.65 V. As is discussed below,  $\text{SO}_2$  seems not to adsorb (or does it very weakly) on gold and therefore it hardly influences the shape of the anodic peak in reverse scans.

The application of in-situ FT-IRRAS to the study of  $\text{SO}_2$  oxidation allows the identification of the reaction products. Fig. 2 shows the spectra obtained at 0.7 and 1.0 V in an  $\text{SO}_2$ -containing 0.5 M  $\text{HClO}_4$ . These spectra resulted from the accumulation and averaging of 200 interferograms and were normalised to a reference spectrum taken at 0.5 V, all in the presence of dissolved  $\text{SO}_2$ . As gleaned from Fig. 2, a consumption of bulk  $\text{SO}_2$  takes place at both potentials (positive band at  $1332 \text{ cm}^{-1}$ ) as a consequence of its transformation into a mixture of hydrogen sulphate (negative bands at  $1200$  and  $1050 \text{ cm}^{-1}$ ) and sulphate (negative band at  $1110 \text{ cm}^{-1}$ ) anions. This latter band could arise alternatively from the asymmetric vibration of perchlorate anions, which may migrate into the thin layer to compensate excess hydrated protons generated during  $\text{SO}_2$  oxidation. However, the spectral analysis of the oxidation of  $\text{SO}_2$  on sulphur-modified Pt electrodes (which feature a diffusion-limited anodic peak located in the double layer potential region) carried out in 0.5 M  $\text{HCl}$  also revealed a clear-cut band at  $1118 \text{ cm}^{-1}$  [14,15]. This result sustains the assignation of this band to a sulphate vibrational mode, yet it could comprise perchlorate vibrational contributions in  $\text{HClO}_4$  solutions. As concluded for the case of Pt [9,10], hydrogen sulphate/sulphate are the stable final product, but the involvement of S(V), i.e. dithionate ions, as a short lifetime intermediate species cannot be ruled out because its character-

istic stretching vibrations ( $\nu_{\text{as}} = 1200\text{--}1240\text{ cm}^{-1}$ ,  $\nu_{\text{s}} = 990\text{--}1090\text{ cm}^{-1}$  [16,17]) can be masked by the larger features of S(VI) species. A recent in situ radiotracer study [6] showed an increase of sulphur surface excess in the region of  $\text{SO}_2$  oxidation, which was indicative of the formation and adsorption of oxidation products. Dithionate was proposed as an intermediate reaction product, which stabilises as a surface complex.

Concerning the possible existence of adsorbed intermediates participating the oxidation mechanism, the occurrence of an anodic post-peak, following the diffusion-like  $\text{SO}_2$  oxidation peak, has been reported [3,4], which was attributed to the oxidation of strongly adsorbed  $\text{SO}_2$ . However, we did not detect such a response in our voltammetric experiments, not even at a high sweep rate ( $200\text{ mV s}^{-1}$ ) in a diluted  $\text{SO}_2$  solution, conditions under which a surface process should become more clearly distinguishable. Moreover, a typical blank voltammogram was recorded after controlled potential adsorption in a 100 mM S(IV) sulphuric acid solution (0.5 V, 2 min) and the transferral of the electrode to an auxiliary cell with  $\text{SO}_2$ -free test solution. This result implies the absence of any stable adsorbed residue, i.e. either the adsorbate is lost during the transfer stage or no adsorption occurs at all. In situ surface-sensitive vibrational spectroscopic techniques were applied in order to make sure of the involvement of an adsorbed species. IR spectroscopy did not show any vibrational band attributable to S–O-like adsorbed residues at the initial potential. Spectra taken with increasing time at 0.5 V in the presence of  $\text{SO}_2$  and normalised to a reference spectrum in the absence of  $\text{SO}_2$  at the same potential showed only the growth of the asymmetric stretch band for dissolved  $\text{SO}_2$  ( $1332\text{ cm}^{-1}$ ). Meanwhile, the baseline noise level remained constant in the spectral range of interest and no additional bands attributable to S–O adsorbed species could be perceived. However, this fact is not sufficient evidence to sustain the absence of a chemisorbed  $\text{SO}_2$  state, since some  $\text{SO}_2$ -transition metal coordination geometries (e.g.  $\eta^1$ -like symmetries, [18]) have IR-active modes lying at frequencies below the typical cut-off of the window material ( $\sim 1000\text{ cm}^{-1}$  for flat  $\text{CaF}_2$  windows).

In contrast, SERS is regarded as the most surface-sensitive vibrational technique operated in situ that combines a wide spectral range ( $100\text{--}5000\text{ cm}^{-1}$ ) with a high resolution [19]. In this instance, SER spectra for a roughened (SER-active) gold substrate in contact with  $\text{SO}_2$ -containing electrolyte at various potentials between 0.5 and 0.3 V/RHE, i.e. above the commencement of reduction of  $\text{SO}_2$  to yield adsorbed sulphur, appeared essentially featureless, especially in the spectral range expected for S–O stretching frequencies ( $900\text{--}1300\text{ cm}^{-1}$ , [17]). Moreover, the spectra were virtually undistinguished from those taken in contact

with the test electrolyte within the same potential range or in air.

The SER monitoring of the  $\text{SO}_2$  oxidation process did not reveal the production of any adsorbable species. The only remarkable feature was the development of a very broad band covering the range  $400\text{--}700\text{ cm}^{-1}$  at potentials higher than 1.4 V. As reported earlier [1,20], this band corresponds to the metal–oxygen vibration of the surface metal oxide. These results conflict with previous data reported by Wilke et al. [5], who studied the adsorption of gas-phase and aqueous  $\text{SO}_2$  on active-SER gold and Pt-, Rh- and Ru-coated gold surfaces. On unmodified gold, these authors found a band at  $1130\text{ cm}^{-1}$  at both the gas–metal and the aqueous–metal electrochemical interfaces (at 0.4 V/SCE or  $\sim 0.64\text{ V/SCE}$ ). This band was assigned to a symmetric S–O stretch for molecularly adsorbed  $\text{SO}_2$ .

In our opinion, the different experimental conditions applied may be at the origin of these discrepancies. One should note that in [5],  $\text{SO}_2$  was admitted into the electrochemical cell by sparging a stream of the pure gas for 10–20 s. Although still the subject of some debate, the total enhanced Raman intensity is believed to arise from molecules chemisorbed on the surface (through an adsorption-induced charge transfer mechanism) and from molecules either physisorbed or situated further away but still close enough to feel the so-called EM effect (amplification of the surface electromagnetic field associated with the development of large-scale metal surface structures) [19,21]. The EM enhancing factor depends on the distribution of the molecules with the distance from the surface of the metal particles, and hence increases with increasing concentration of the scattering species [19]. Sparging pure  $\text{SO}_2$  into the working solution could result in a higher  $\text{SO}_2$  concentration than that used in this work. On the other hand, band assignment in potential-dependent SER experiments was made in [5] by comparison with the behaviour found in the gas-phase system. During the study of gas-phase  $\text{SO}_2$  adsorption, it was clear that the  $1130\text{ cm}^{-1}$  band disappears when  $\text{SO}_2$  is pumped out of the chamber. This reversible behaviour is commonly regarded as an evidence of a physical interaction between the adsorbate and the substrate (i.e. physisorption) rather than a true surface bonding (i.e. chemisorption). The adsorption/desorption of gas  $\text{SO}_2$  on several porous substrates (e.g. carbons [22], alumina [23–25] and zeolites [25,26]) has been frequently dealt with by using IR spectroscopy as the characterisation tool. Several authors reported a vibrational band ranging from  $1150$  to  $1120\text{ cm}^{-1}$  when the surface is exposed to a 0.2–2%  $\text{SO}_2$  feed at atmospheric base pressure and room temperature. This feature was assigned to a physisorbed  $\text{SO}_2$  state, as supported by the disappearance of the band upon  $\text{SO}_2$  evacuation. Moreover, HREELS (High Resolution Electron Energy Loss

Spectroscopy) studies of SO<sub>2</sub> adsorption on noble metal surfaces under UHV environment [27–30] showed a vibration at  $\sim 1140\text{ cm}^{-1}$  for (physisorbed) SO<sub>2</sub> multilayers. Thus, it is feasible that physisorbed molecular SO<sub>2</sub> formed on the roughened gold surface in Wilke's experiments and the EM effect becomes the major contribution to the enhanced Raman signal. In summary, the results discussed so far strongly suggest that the oxidation of bulk SO<sub>2</sub> seems not to proceed on a surface with strongly adsorbed SO<sub>2</sub>.

### 3.2. Electrocatalysis by sulphur-modified gold electrodes

Samec and Weber [3,4] reported a considerable enhancement of the SO<sub>2</sub> oxidation reaction (manifested by a 50–100-mV shift of the current peak to less positive potentials) after a preliminary voltammetric cycle to potentials encompassing SO<sub>2</sub> reduction. This enhancement was correlated to a 70% coverage by the so-called 'adsorbed reduced species' (assumed to be S and H<sub>2</sub>S). In a previous work [1], we postulated that SO<sub>2</sub> reduces on gold to form a monolayer of monomeric sulphur and soluble S(-II) species. These latter species re-oxidise and deposit as a multilayer of polymeric sulphur. In accord with this view, the promotion of the SO<sub>2</sub> oxidation reaction should be entirely attributed to a sulphur adlayer. Sulphur is known to alter the catalytic properties of many metals and influence the course of a number of electrochemical reactions, such as the oxidation of small organic molecules [31,32] and the reduction of nitric oxide [33]. Also, the catalytic effect of adsorbed sulphur on the oxidation of SO<sub>2</sub> at platinum electrodes is well established [8,11]; catalysis is effected provided critical sulphur coverage is not exceeded, since excess sulphur renders the layer inhibiting. A study of the catalytic/poisoning properties of sulphur adlayers has been also undertaken in this work.

As reported in a precedent paper [1], the coverage of sulphur adlayers formed in a SO<sub>2</sub>-containing solution after a single cycle  $0.5 \rightarrow E_{\text{low}} \rightarrow 0.55\text{ V}$  can be controlled by setting  $E_{\text{low}}$  to an adequate value. The so-formed adlayer can be isolated as usual and characterised voltammetrically in the desired test electrolyte. Typical voltammograms for the stripping of the so-formed adlayers are displayed in Fig. 3. In all cases (Fig. 3(a–f)), the complete removal of the sulphur adlayer is attained in a single cycle after which the characteristic profile for a blank voltammogram (not shown) is recovered. Sulphur coverages were calculated from the sulphur oxidation charge, taken as the difference between the total oxidation charge and the charge for the reduction of the surface metal oxide. As expected, sulphur coverage increases upon lowering  $E_{\text{low}}$ . The characteristic sulphur oxidation peaks, namely, O<sub>2</sub> associated with the oxidation of monomeric adsorbed

sulphur and O<sub>1</sub> related to the desorption of polymeric adsorbed sulphur, can be distinguished in the set of voltammograms in Fig. 3. As anticipated in a precedent paper [1], peak O<sub>1</sub> grows and shifts positively with increasing coverage, eventually overlapping peak O<sub>2</sub>. This behaviour is consistent with the fact that deposition of multilayer sulphur occurs on top of the first chemisorbed layer.

Fig. 4 shows the effect of sulphur coverage on the kinetics of the SO<sub>2</sub> oxidation reaction on sulphur-modified gold electrodes. Sulphur adlayers of various coverages were generated in situ during a sweep down to a lower potential limit ( $E_{\text{low}}$ , set in accord with results depicted in Fig. 3) and reversal to 1.75 V. The first negative cycle is not depicted for clarity. The catalytic properties of the so-formed sulphur adlayers towards the electro-oxidation of SO<sub>2</sub> were assessed by monitoring the potential shift ( $\Delta E_p = E_{p,\theta} - E_{p,0}$ , where subscript  $\theta$  refers to gold electrodes modified by sulphur adsorbed at a coverage  $\theta$  and subscript 0 corresponds to the unmodified surface) and the normalised peak current ( $j_{p,\theta}/j_{p,0}$ ) of the diffusion-limited SO<sub>2</sub> oxidation peak. The evolution of these parameters is plotted as a function of sulphur coverage in Figs. 5 and 6 for a 10 mM S(IV) + 10% H<sub>2</sub>SO<sub>4</sub> working solution. From Figs. 4 and 5, it follows that the SO<sub>2</sub> oxidation peak shifts to lower potentials as the coverage increases. Once a coverage of  $\sim 0.5$  is exceeded, the oxidation peak shifts back. The peak current barely changes for sulphur coverages up to  $\sim 0.75$ , but undergoes a dramatic diminution until its complete suppression at higher coverages. In addition, a parallel development of higher potential anodic features related to desorption of the sulphur adsorbed layer and oxidation of SO<sub>2</sub> on fresh bare sites is observed (Fig. 4). Taking into account the variation in both of these parameters, it can be concluded that sulphur adlayers with coverage close to 0.5 are the most efficient for the electro-oxidation of SO<sub>2</sub>. Higher coverage sulphur layers gradually render the surface inhibiting towards SO<sub>2</sub> oxidation. From saturation coverage values found in gold single crystals under UHV conditions (0.59, 0.52 and 0.41 for the (111), (100) and (110) orientations, respectively [34]), it can be postulated that 0.5 approximately corresponds to the completion of a monolayer of chemisorbed monomeric sulphur.

Catalysis/inhibition exercised by adlayers produced ex situ from sulphide adsorption in acidic (Figs. 5 and 6, open circle) and alkaline media (Figs. 5 and 6, open triangle) was also tested. These layers were generated in  $5 \times 10^{-5} - 10^{-3}\text{ M S(-II)}$  solutions by scanning from a given lower potential limit ( $-0.15\text{ V/RHE}$  in acidic medium and  $-0.25\text{ V/RHE}$  in alkaline medium) to an increasing upper potential limit. The so-formed adlayers were isolated by rinsing with ultrapure water and their catalytic properties tested in a 10 mM S(IV) +

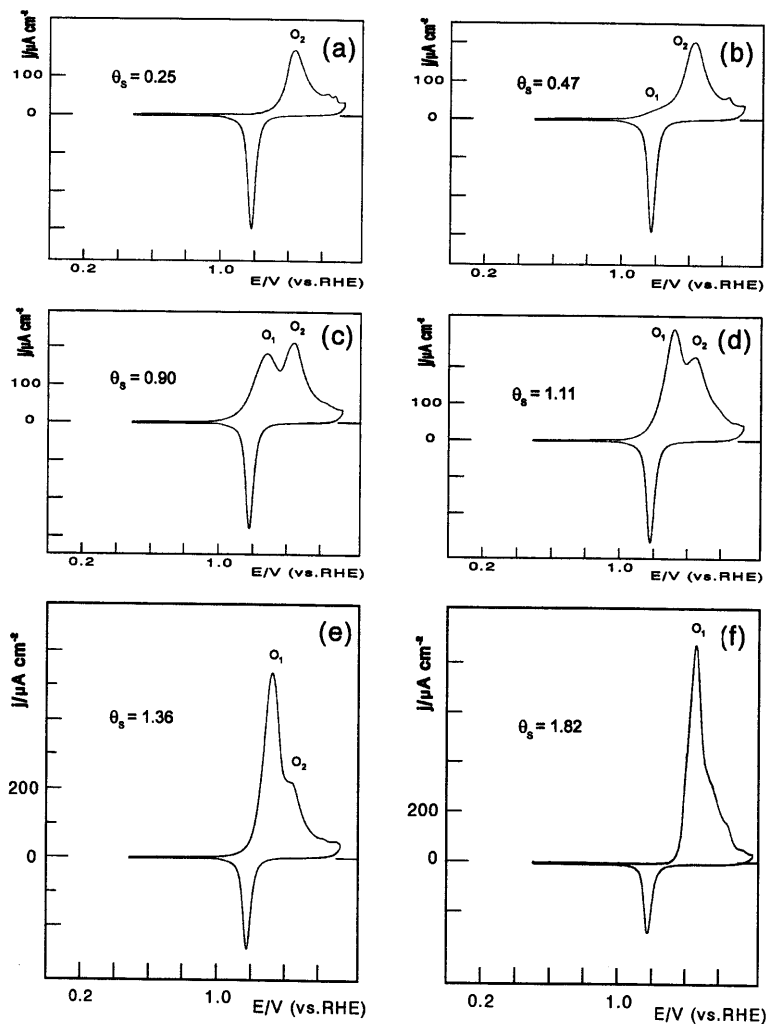


Fig. 3. Oxidative stripping of adsorbed sulphur formed on gold by in situ reduction of  $\text{SO}_2$  ( $0.5 \rightarrow E_{\text{low}} \rightarrow 0.55$  V).  $E_{\text{low}}$  = (a) 0.1, (b) 0.0, (c)  $-0.035$ , (d)  $-0.05$ , (e)  $-0.10$ , and (f)  $-0.20$  V, respectively. Supporting electrolyte: 10 %  $\text{H}_2\text{SO}_4$ .

10%  $\text{H}_2\text{SO}_4$  (Figs. 5 and 6). The coverage-dependence of the peak shift and normalised current peak for these ex situ adlayers fits that exhibited by in situ adlayers derived from  $\text{SO}_2$  transformation. Therefore, 0.5 appears to be the optimum surface coverage value for maximum catalysis, regardless of the adlayer generation method employed. The matching of data depicted in Figs. 5 and 6 supports the hypothesis put forward in part I [1] of the existence of a close link between the oxidative and the reductive behaviours of sulphide and sulphur dioxide respectively, both involving common adsorbed species. This statement is particularly true for monomeric sulphur adlayers which exhibit identical chemical, structural and catalytic properties.

FT-IR was used to check whether or not production of new chemical species on the sulphur-modified gold surface is connected with enhanced or inhibited  $\text{SO}_2$

oxidation. The spectroscopic analysis was carried out for the oxidation of  $\text{SO}_2$  at 1.0 V on several sulphur-modified substrates with increasing  $\theta_s$  formed by previous cycles to 0.1 V, 0.0 and  $-0.05$  V respectively in the same  $\text{SO}_2$ -containing working solution. No noticeable differences were encountered between spectra for catalysed oxidations (sulphur layers formed after cycling down to 0.1 or 0.0 V, respectively) and those in Fig. 2. The only remarkable result was that the  $\text{SO}_2$  consumption and the S(VI) generation bands were barely discerned for high coverage S–Au electrodes, as expected owing to the strong inhibiting properties of the layer.

Finally, a brief comparison between the electrocatalytic performance of Pt and Au electrodes towards  $\text{SO}_2$  is pertinent to the present discussion. Recent voltammetric and in situ infrared data [9,10] have shown that

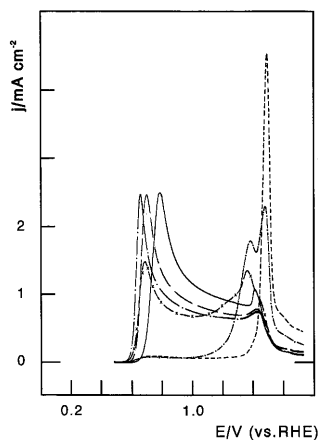


Fig. 4. Electrocatalysis of  $\text{SO}_2$  oxidation on sulphur-modified gold electrodes;  $\theta_{\text{S}} = 0$  (—), 0.25 (---), 0.47 (— · —), 1.11 (— × —), 1.36 (— · —) and 1.82 (----). Adsorbed sulphur was generated in situ by excursions to various potentials below 0.5 V/RHE (not shown). Supporting electrolyte: 10 %  $\text{H}_2\text{SO}_4$ ;  $c_{\text{S(IV)}} = 10$  mM.

$\text{SO}_2$  strongly adsorbs on Pt at open circuit or at double-layer potential. Adsorbed  $\text{SO}_2$  has been suggested to induce a large deactivation of the Pt surface and be responsible for the inhibition of the ‘diffusion-limited’ oxidation of bulk  $\text{SO}_2$ , so restricting the process to the oxygen adsorption region of Pt [9,10]. The generation of sulphur adlayers of increasing coverage on the Pt surface was shown to be accompanied by the development of a  $\text{SO}_2$  oxidation mode at double layer poten-

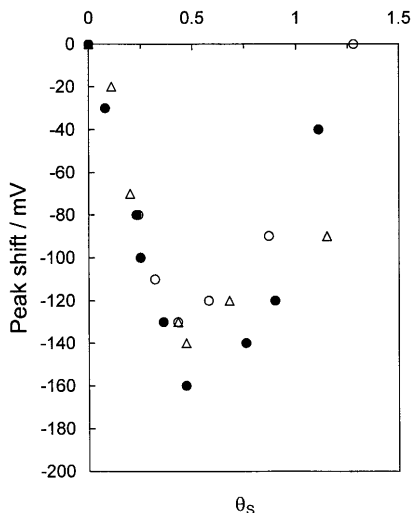


Fig. 5. Plot of the  $\text{SO}_2$  oxidation peak shift vs. sulphur coverage for 10 mM  $\text{S(IV)} + 10$  %  $\text{H}_2\text{SO}_4$ . The adlayers were generated in situ in the same working solution (●), ex situ in  $\text{S(II)} + 0.5$  M  $\text{H}_2\text{SO}_4$  (○) and ex situ in  $\text{S(II)} + 0.1$  M  $\text{NaOH}$  (△).

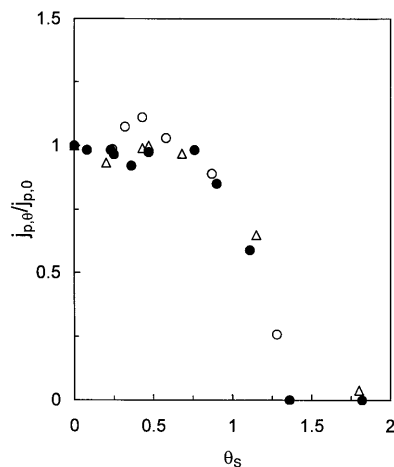


Fig. 6. Plot of the normalised peak current vs. sulphur coverage for 10 mM  $\text{S(IV)} + 10$  %  $\text{H}_2\text{SO}_4$ . The adlayers were generated in situ in the same working solution (●), ex situ in  $\text{S(II)} + 0.5$  M  $\text{H}_2\text{SO}_4$  (○) and ex situ in  $\text{S(II)} + 0.1$  M  $\text{NaOH}$  (△).

tials [9–11], thus effecting a considerable promotion of the  $\text{SO}_2$  oxidation reaction. This oxidation mode eventually features a diffusion-limited shape, comparable to that described in this work (Fig. 1). Catalysis exercised by adsorbed sulphur on Pt was interpreted in terms of preclusion of detrimental  $\text{SO}_2$  adsorption, although enhancement by intrinsic sulphur catalysis, i.e. activation of sulphur neighbouring sites through surface electronic interactions, could not be ruled out [10,35]. By contrast, it follows from the discussion in section 3.1 that the oxidation of bulk  $\text{SO}_2$  on Au proceeds on a bare surface or at most on a surface with weakly adsorbed  $\text{SO}_2$ . The absence of strongly adsorbed  $\text{SO}_2$  most likely permits unmodified gold electrodes to show substantial intrinsic electrocatalysis towards  $\text{SO}_2$  oxidation. Under this assumption, improved kinetics on sulphur-modified Au electrodes may be related to the capability of this adatom to modify the surface electronic distribution of adjacent sites.

### 3.3. Overall electrochemical behaviour of $\text{SO}_2$

The voltammetric and spectroscopic data addressed in part I of this series and in the present paper provide a deeper understanding of the electrochemical reactivity of  $\text{SO}_2$  and related adsorbed species on Au. At this juncture, the various features observed in a voltammogram recorded over a wide potential window (comprising both oxidation and reduction) can be unambiguously assigned to either bulk or surface processes.

The voltammogram in Fig. 7 illustrates the overall behaviour of  $\text{SO}_2$  on gold. The initial potential was set

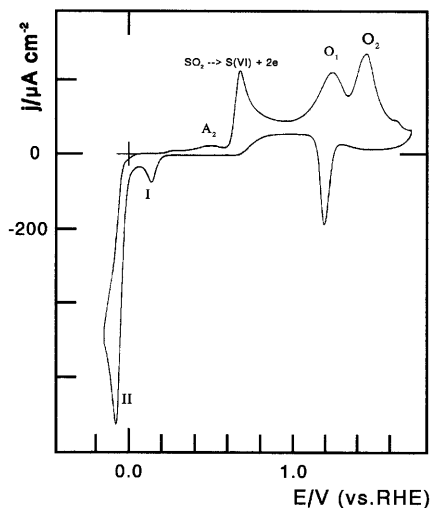


Fig. 7. Overall voltammetric behaviour of aqueous  $\text{SO}_2$  on polycrystalline gold in 10 %  $\text{H}_2\text{SO}_4$ ;  $c_{\text{S(IV)}} = 1 \text{ mM}$ ,  $E_i = 0.5 \text{ V}$ . Polarisation programme:  $0.5 \rightarrow -0.15 \rightarrow 1.75 \rightarrow 0.5 \text{ V}$ .

at 0.5 V/RHE and a periodic potential programme,  $0.5 \rightarrow -0.15 \rightarrow 1.75 \rightarrow 0.5 \text{ V}$ , was applied. From knowledge of the electrochemical reactivity of  $\text{SO}_2$  gained so far, the cathodic peak at 0.14 V/RHE (I) corresponds to the formation of monomeric adsorbed sulphur and the peak at  $-0.075 \text{ V}$  (II) can be assigned to reduction of bulk  $\text{SO}_2$  to soluble S(-II) species. The waves associated with the formation of polymeric sulphur multilayers via oxidation of products of bulk  $\text{SO}_2$  reduction are also discerned on the anodic sweep (and denoted  $A_2$ ), followed by the oxidation of bulk  $\text{SO}_2$  (0.68 V) and the peaks for the stripping of sulphur multilayers ( $O_1$ ) and the underlying monomeric sulphur layer ( $O_2$ ). Oxygen adsorption occurs simultaneously under peak  $O_2$  and desorbs on the reverse scan at  $\sim 1.2 \text{ V}$ .

#### 4. Conclusions

Polycrystalline gold electrodes exhibit good intrinsic electrocatalytic response towards the oxidation of aqueous  $\text{SO}_2$  in acidic media. The oxidation reaction starts at potentials slightly higher than 0.6 V displaying a characteristic voltammetric peak for irreversible processes whose maximum rate is diffusion limited. The absence of S–O stretching vibrations in IR and, above all, in SER spectra respectively suggests that  $\text{SO}_2$  does not strongly adsorb on this metallic substrate. The poor capability of gold as  $\text{SO}_2$  chemisorber allows the deleterious effect of this adsorbed species on the kinetics of the bulk oxidation process to be avoided. In contrast, the adsorption of  $\text{SO}_2$  was found to play a dominant role in the behaviour of Pt electrodes to  $\text{SO}_2$  oxidation [9]. On the other hand, adsorption of sulphur brings

about a significant enhancement of the  $\text{SO}_2$  oxidation reaction (Fig. 4). Maximum efficiency is reached at  $\theta_S \sim 0.5$ , which appears to be close to a full monolayer of monomeric sulphur. At higher sulphur coverages, the electrode gradually undergoes a loss of the electrocatalytic activity until a complete inhibition of the  $\text{SO}_2$  oxidation reaction is attained.

As a final conclusion, it should be stressed that gold exhibits a far better performance towards  $\text{SO}_2$  oxidation when compared to platinum. Thus, it is rather surprising that platinum has been largely preferred as the electrocatalytic material for the electrochemical oxidation of  $\text{SO}_2$ .

#### Acknowledgements

The authors would like to thank Dr S. Cooper (Strathclyde) for her advice and instruction in the use of the Raman Microscope facility and to Dr F.J. Huerta (Alicante) for his help in FT-IR data collection. C. Quijada and E. Morallón are indebted to the ‘Ministerio de Educación y Cultura’ for the award of their F.P.I. postdoctoral fellowships. Financial support from the ‘Instituto de Cultura J. Gil Albert’ and from the ‘Ministerio de Educación y Cultura’ (contract PB97-0130) is gratefully acknowledged.

#### References

- [1] C. Quijada, F.J. Huerta, E. Morallón, J.L. Vázquez, L.E.A. Berlouis, *Electrochim. Acta* 45 (1847) 2000.
- [2] E.T. Seo, D.T. Sawyer, *Electrochim. Acta* 10 (1965) 239.
- [3] Z. Samec, J. Weber, *Electrochim. Acta* 20 (1975) 403.
- [4] Z. Samec, J. Weber, *Electrochim. Acta* 20 (1975) 413.
- [5] T. Wilke, X. Gao, C.G. Takoudis, M.J. Weaver, *J. Catal.* 130 (1991) 62.
- [6] K. Varga, P. Baradlai, A. Vertes, *Electrochim. Acta* 42 (1997) 1143.
- [7] M. Comtat, J. Mahenc, *Bull. Soc. Chim. Fr.* 11 (1969) 3862.
- [8] R.M. Spotnitz, J.A. Colucci, S.H. Langer, *Electrochim. Acta* 28 (1983) 1053.
- [9] C. Quijada, A. Rodes, J.L. Vázquez, J.M. Pérez, A. Aldaz, *J. Electroanal. Chem.* 394 (1995) 217.
- [10] C. Quijada, A. Rodes, J.L. Vázquez, J.M. Pérez, A. Aldaz, *J. Electroanal. Chem.* 398 (1995) 105.
- [11] C. Quijada, J.L. Vázquez, A. Aldaz, *J. Electroanal. Chem.* 414 (1996) 229.
- [12] J.M. Feliu, J. Claret, C. Muller, J.L. Vázquez, A. Aldaz, *J. Electroanal. Chem.* 197 (1984) 271.
- [13] G. Codina, G. Sánchez, A. Aldaz, *Electrochim. Acta* 36 (1991) 1129.
- [14] C. Quijada. PhD. Thesis, Universidad de Alicante, 1997.
- [15] C. Quijada, J.L. Vázquez, F.J. Vicent, to be submitted to *Recent Research Developments in Electrochemistry*.
- [16] W.G. Palmer, *J. Chem. Soc.* 1552 (1961).



- [17] A.J. Banister, L.F. Moore, J.S. Padley, in: G. Nickless (Ed.), *Inorganic Sulphur Chemistry*, chapter 5, Elsevier, Amsterdam, 1968.
- [18] R.R. Ryan, G.J. Kubas, D.C. Moody, P.G. Eller, *Struct. Bonding* 46 (1981) 47.
- [19] R.L. Birke, J.R. Lombardi, in: R.J. Gale (Ed.), *Spectroelectrochemistry. Theory and Practice*, chapter 6, Plenum Press, New York, 1988.
- [20] J. Desilvestro, M.J. Weaver, *J. Electroanal. Chem.* 209 (1987) 377.
- [21] R.E. Hester, in: R.G. Compton, A. Hamnett (Eds.), *Comprehensive Chemical Kinetics. New Techniques for the study of electrodes and their reactions*, chapter 2, vol. 29, Elsevier, Amsterdam, 1989.
- [22] J. Zawadzki, *Carbon* 25 (1987) 495.
- [23] A.V. Deo, I.G. Dalla Lana, H.W. Habgood, *J. Catal.* 21 (1971) 270.
- [24] H.G. Karge, I.G. Dalla Lana, *J. Phys. Chem.* 88 (1984) 1538.
- [25] H.G. Karge, *Proceedings of the Tenth National Symposium on Catalysis and Fourth Indo-Soviet Seminar on Catalysis*, December 18–21, Madras, India, 1990.
- [26] J. García-Martínez, MSc Thesis. Universidad de Alicante, 1998.
- [27] D.A. Outka, R.J. Madix, G.B. Fisher, C. DiMaggio, *J. Phys. Chem.* 90 (1986) 4051.
- [28] M.L. Burke, R.J. Madix, *Surf. Sci.* 194 (1988) 223.
- [29] M.L. Burke, R.J. Madix, *J. Phys. Chem.* 92 (1974) 1988.
- [30] Y.-M. Sun, D. Sloan, D.J. Albers, M. Kovar, Z.-J. Sun, J.M. White, *Surf. Sci.* 319 (1994) 34.
- [31] T. Loucka, *J. Electroanal. Chem.* 36 (1972) 355.
- [32] R. Jarayam, A.Q. Contractor, H. Lal, *J. Electroanal. Chem.* 87 (1978) 225.
- [33] M.J. Foral, S.H. Langer, *Electrochim. Acta* 33 (1988) 257.
- [34] M. Kostelitz, J.L. Domange, J. Oudar, *Surf. Sci.* 34 (1973) 431.
- [35] M.J. Foral, S.H. Langer, *J. Electroanal. Chem.* 246 (1988) 193.